

# Modeling High-energy and Very-high-energy $\gamma$ -rays from the Terzan 5 Cluster

Christo Venter<sup>1</sup>, Ocker C. de Jager<sup>1</sup>, Andreas Kopp<sup>2</sup>, Ingo Buesching<sup>3</sup>, & André-Claude Clapson<sup>4</sup>

<sup>1</sup> Centre for Space Research, North-West University, Potchefstroom Campus, Private Bag X6001, Potchefstroom, 2520, South Africa  
<sup>2</sup> Institut für Experimentelle und Angewandte Physik, Christian-Albrechts-Universität zu Kiel, Leibnizstrasse 11, 24118 Kiel, Germany  
<sup>3</sup> Institut für Theoretische Physik, Lehrstuhl IV: Weltraum- und Astrophysik, Ruhr-Universität Bochum, 44780 Bochum, Germany  
<sup>4</sup> Max-Planck-Institut für Kernphysik, PO Box 103980, 69029 Heidelberg, Germany

## Abstract:

*Fermi* Large Area Telescope (LAT) has recently detected a population of globular clusters (GCs) in high-energy (HE)  $\gamma$ -rays. Their spectral properties and energetics are consistent with cumulative emission from a population of millisecond pulsars (MSPs) hosted by these clusters. For example, the HE spectra exhibit fairly hard power-law indices and cutoffs around a few GeV, typical of pulsed spectra measured for the  $\gamma$ -ray pulsar population. The energetics may be used to constrain the number of visible MSPs in the cluster ( $N_{vis}$ ), assuming canonical values for the average  $\gamma$ -ray efficiency and spin-down power. This interpretation is indeed strengthened by the fact that the first  $\gamma$ -ray MSP has now been identified in the GC NGC 6624 [9]. On the other hand, it has been argued that the MSPs are also sources of relativistic leptons which may be reaccelerated in shocks originating in collisions of stellar winds in the cluster core, and may upscatter bright starlight and cosmic microwave background photons to very high energies. Therefore, this unpulsed component may give an independent constraint on the number of MSPs ( $N_{tot}$ ), for a given cluster B-field and diffusion coefficient. Lastly, the transport properties of the energetic leptons may be further constrained using multiwavelength data, e.g., to infer the radial dependence of the diffusion coefficient and cluster B-field. We present results on our modeling of the pulsed and unpulsed  $\gamma$ -ray fluxes from the GC Terzan 5.

## Introduction

The recent *Fermi* LAT detection of several globular clusters (GCs) in HE [1,2,7,10] underlined the importance of modeling collective  $\gamma$ -ray emission of millisecond pulsars (MSPs) in GCs. In addition, a steady flux from such populations is also expected in the VHE domain [3,4,12,14]. We present pulsed curvature radiation (CR) as well as unpulsed inverse Compton (IC) calculations for an ensemble of MSPs in the GC Terzan 5. Using both the pulsed HE and unpulsed VHE components, independent constraints may be derived on the total number of MSPs ( $N_{tot}$ ), while the nebular B-field may be constrained using synchrotron radiation (SR) and IC flux components.

## Model

We have previously calculated the pulsed CR spectrum resulting from relativistic leptons which are accelerated in the MSP magnetospheres by large pair-starved E-fields, and constrained to move along curved B-lines [13]. We also calculate an unpulsed flux component, using a cumulative injection spectrum made up of electrons leaving the MSP magnetospheres after having been accelerated by the pair-starved magnetospheric E-fields, and neglecting reacceleration.

Using updated structural parameters, a much larger bolometric luminosity, and a distance of  $d = 5.5$  kpc [5,8,11], we calculate the radiation losses and resulting unpulsed IC fluxes (see Fig. 1) assuming Bohm diffusion and B-fields of  $B = 1 \mu\text{G}$  and  $B = 10 \mu\text{G}$ . We used two radiation zones in the cluster: a core region extending from  $r = 0$  up to the core radius, as well as a halo region extending from the core radius up to the tidal

radius. We used both bright starlight and CMB as soft photon targets. The energy density of the first was assumed to be  $\sim 2.4 \times 10^4 \text{ eV/cm}^3$  and  $\sim 1.6 \times 10^3 \text{ eV/cm}^3$  for each of the regions (for a temperature  $T = 4500 \text{ K}$ , and due to large stellar luminosity and small core radius), while the energy density for the CMB was taken to be  $\sim 0.27 \text{ eV/cm}^3$  (for  $T = 2.76 \text{ K}$ ).

## Results

Scaling the pulsed CR component [14] to fit the *Fermi* LAT data [2] implies that the number of visible MSPs  $N_{vis} \sim 60 \pm 30$ . This is consistent with the estimate of  $180^{+90}_{-100}$  obtained by [2], and formally presents a lower limit for  $N_{tot}$ . However, the pair-starved model probably overpredicts the CR flux by a factor of a few, and furthermore may not be valid for all MSPs (as inferred from light curve modeling [15]), so that the first number should likely be larger.

Provided that the High Energy Stereoscopic System (H.E.S.S.) does not see Terzan 5, one can use both the HE data and VHE upper limits to constrain  $N_{tot}$  (since  $N_{tot} \geq N_{vis}$ ) and the cluster

B-field (see Fig. 2). A H.E.S.S. detection may however imply less severe constraints on  $N_{tot}$ , while the Cherenkov Telescope Array (CTA) will provide much more stringent future constraints.

## Conclusion

One may derive important system constraints on Terzan 5 by using multiwavelength data. Future work include attempts to constrain the radial profile of the diffusion coefficient and cluster field  $B$  using radio and X-ray observations.

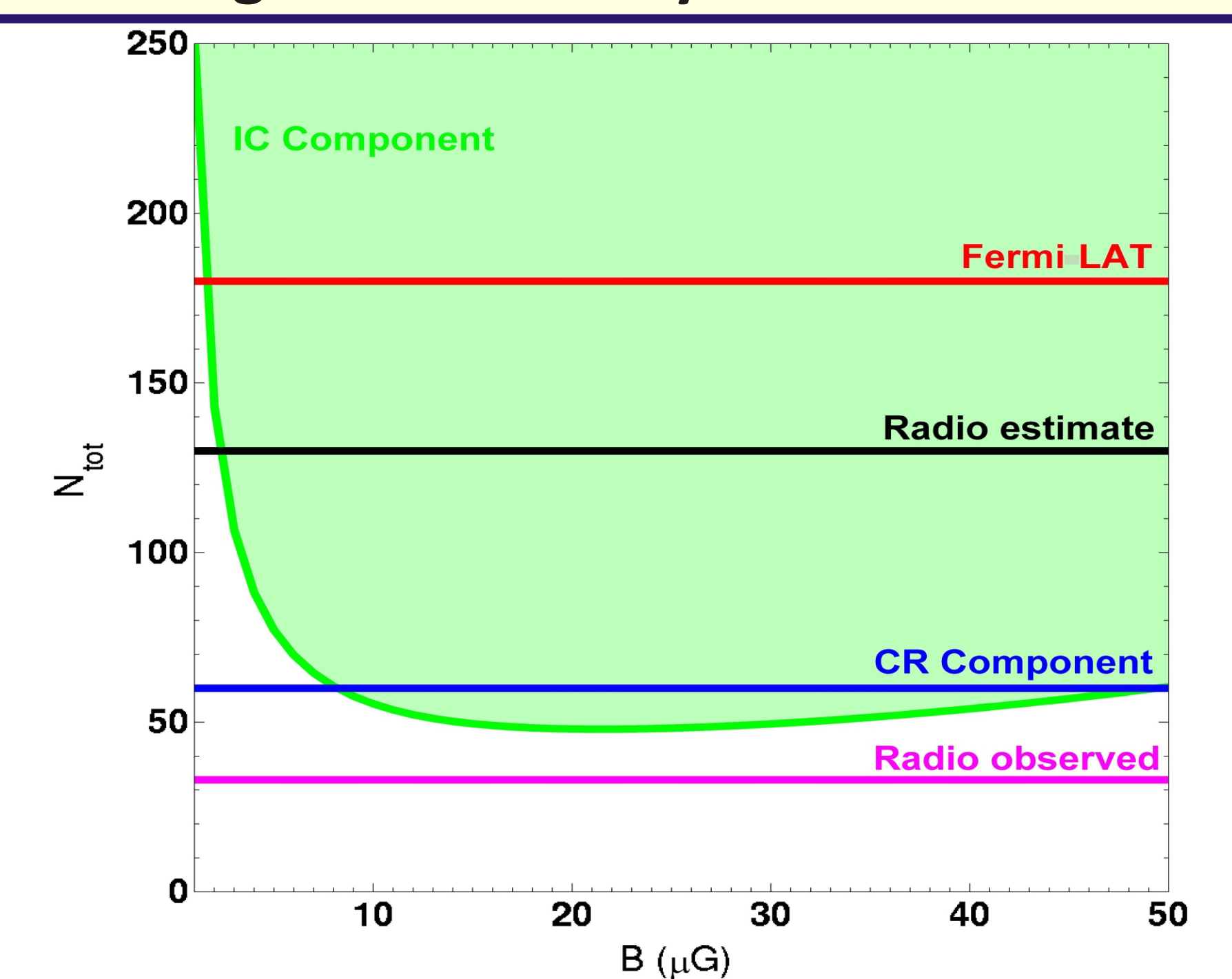


Figure 2. Constraints on  $N_{tot}$  vs.  $B$ . Green line: ICS component using H.E.S.S. sensitivity (this work; light green area is excluded). Red and blue lines:  $N_{vis}$  from [2] and this work (CR component); magenta and black lines: number of radio MSPs detected and estimated [6]. Errors not shown.

## References

- [1] Abdo, A. A. et al. 2009, *Science*, 325, 845
- [2] Abdo, A. A. et al. 2010, *A&A*, 524, 75
- [3] Bednarek, W., & Sitarek, J. 2007, *MNRAS*, 377, 920
- [4] Cheng, K.S. et al. 2011, *ApJ*, 723, 1219
- [5] Ferraro, F. R. et al. 2009, *Nature*, 462, 483
- [6] Fruchter, A. S., & Goss, W. M. 2000, *ApJ*, 536, 865
- [7] Kong, A. K. H., Hui, C. Y., & Cheng, K.S. 2010, *ApJL*, 712, 36
- [8] Lanzoni, B. et al. 2010, *ApJ*, 717, 653
- [9] Parent, D., Poster presented at this Symposium
- [10] Tam, P.H.T. et al. 2011, *ApJ*, 729, 90
- [11] Valenti, E. et al. 2007, *AJ*, 133, 1287
- [12] Venter, C., & de Jager, O. C. 2008, *AIP Conf. Ser.*, 1085, 277
- [13] Venter, C., & de Jager, O.C. 2008, *ApJ*, 680, L125
- [14] Venter et al. 2009, *ApJL*, 696, 52
- [15] Venter et al. 2009, *ApJ*, 707, 800

This research is based upon work supported by the South African National Research Foundation.

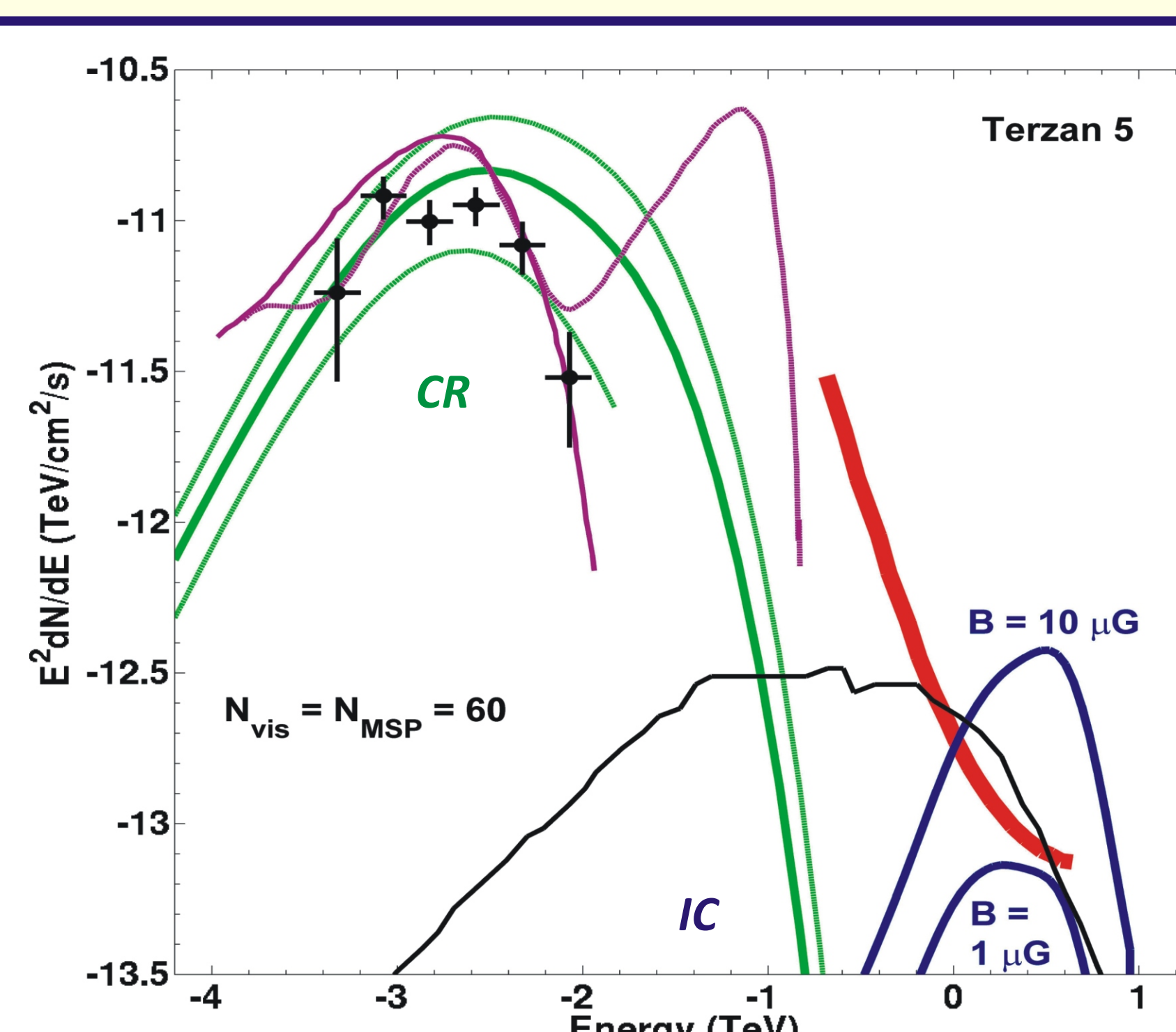


Figure 1. Differential CR and IC spectra for Terzan 5. Green: scaled CR spectrum & errors from [14]; magenta: IC models from [4]; Fermi LAT data [2]; blue: IC spectrum (this work) and black scaled from [3]; red: H.E.S.S. Sensitivity.